



OPEN The value of acetylation reader YEATS2 in hepatocellular carcinoma management

Yongjie Shi^{1,4}, Qiwen Xiao^{1,4}, Weichun Xiao², Jiale Kang¹, Qiang Zhou¹, Hongyun Jia¹✉, Yimei Chen³✉ & Sicong Huang¹✉

Hepatocellular carcinoma (HCC) is frequently associated with Yeats-domain containing 2 (YEATS2) overexpression, which enhances tumor progression via the PI3K/AKT pathway. Our study delineates YEATS2's oncogenic functions in HCC and its potential as a prognostic and predictive biomarker. Through comprehensive *in vitro* and bioinformatics analyses, we reveal that YEATS2 promotes cell proliferation, invasion, and epithelial-mesenchymal transition (EMT). Additionally, YEATS2 modulates the tumor immune microenvironment and predicts response to immunotherapies and chemotherapies. YEATS2's serum stability suggests its utility as a non-invasive biomarker for personalized HCC treatment.

Keywords YEATS2, Hepatocellular carcinoma, Oncogenesis, Treatment strategies

HCC ranks among the most common and deadly cancers globally, with both incidence and mortality rates on the rise in recent years. Despite advances in diagnostics and therapeutic interventions, overall survival rates remain dismal, primarily because recurrence and metastasis account for 90% of patient mortality^{1,2}. Targeted and immunotherapies, aimed at specific genes or signaling pathways, present promising avenues for treatment³. A deeper understanding of the molecular mechanisms underlying HCC, especially identifying specific, sensitive biomarkers, is crucial for early diagnosis, prognosis evaluation, and effective treatment strategies.

Histone acetylation is a critical epigenetic regulatory mechanism that controls gene expression by altering chromatin structure and transcriptional states⁴. Histone acetyltransferases and histone deacetylases maintain a dynamic equilibrium in this process, whose dysregulation can drive aberrant transcriptional programs that promote the onset and progression of HCC⁵. In this regard, YEATS2 has emerged as a focal research subject. As a scaffold subunit of the ADA-2-a complex, it plays a pivotal role in regulating histone acetylation. Previous studies have shown that overexpression of YEATS2 can enhance cell proliferation and migration in various cancers^{6–8}. Recent findings confirm that YEATS2 is upregulated in HCC⁹, where it activates the PI3K/AKT pathway, reshapes the extracellular matrix, and boosts the proliferation, migration, and metastasis of HCC cells¹⁰. Knockdown of YEATS2 expression leads to DNA damage, cellular senescence, and increased NK cell count, significantly reducing tumor volume and weight, indicating that targeting YEATS2 could effectively inhibit HCC growth¹¹.

This study delves into the pivotal role and underlying mechanisms of YEATS2, an acetylation-associated gene, in HCC. Employing rigorous bioinformatic analyses and *in vitro* experimentation, we validate YEATS2's proliferative and invasive effects on HCC cells. Moreover, we elucidate its regulation of immune cell infiltration within the tumor microenvironment and its implications for immunotherapy responsiveness. Multi-faceted analyses of biological datasets and HCC patient specimens confirm YEATS2's overexpression (serum and tissue) as an emerging biomarker for HCC diagnosis, progression tracking, and prognosis prediction^{9–11}. Further, *in vitro*, assays underscore YEATS2's potent contribution to fostering oncogenic traits such as proliferation, invasion, migration, and EMT in HCC cells. These discoveries lay a solid groundwork for advancing YEATS2-targeted strategies in HCC management.

¹Department of Clinical Laboratory, The Second Affiliated Hospital, Guangzhou Medical University, Guangzhou, Guangdong, China. ²The Second Affiliated Hospital, Guangzhou Medical University, Guangzhou, Guangdong, China. ³Physical Examination Center, The Second Affiliated Hospital, Guangzhou Medical University, Guangzhou, Guangdong, China. ⁴Yongjie Shi and Qiwen Xiao contributed equally to this work. ✉email: 2010682001@gzhmu.edu.cn; 2017682034@gzhmu.edu.cn; 2018682005@gzhmu.edu.cn

Materials and methods

Screening of acetylation-related genes

We obtained 240 acetylation-related genes from the Molecular Signatures Database (MSigDB) (<https://www.gsea-msigdb.org/gsea/msigdb/>, accessed March 19, 2024)¹² (Supplementary TableS1). For 377 HCC patients from The Cancer Genome Atlas (TCGA) database (<https://portal.gdc.cancer.gov>)¹³, we processed the RNA-seq data (Transcripts Per Million, TPM) generated by the STAR pipeline from the TCGA-LIHC project along with corresponding clinical information. After excluding normal samples and cases lacking clinical data, we performed log₂ (value + 1) transformation on the expression data. The differentially expressed genes (DEGs) analysis identified significantly altered genes, which were subsequently analyzed using Lasso regression with cross-validation and Cox proportional hazards regression to determine their association with recurrence-free survival (RFS). DESeq2 analyzed differential gene expression¹⁴ with significance set at an adjusted *P*-value < 0.05 and |Log₂FC| ≥ 0.93. All statistical analyses were conducted using R (version 4.2.1), with data visualization performed using the ggplot2 package.

Correlation of YEATS2 expression and clinical pathological features

The data were obtained from the Biomarker Exploration for Solid Tumors (BEST) database¹⁵. mRNA-seq data were converted to TPM values and were visualized through box plots. YEATS2 expression levels were compared among clinical groups using either the Wilcoxon rank-sum test or the Kruskal-Wallis test, depending on the number of groups being compared. Survival differences were evaluated by Kaplan-Meier survival curves, with statistical significance being determined through log-rank tests. The diagnostic value was assessed by constructing receiver operating characteristic (ROC) curves, where the area under the curve (AUC) was calculated.

Human HCC tissue and peripheral blood samples

This study utilized 9 snap-frozen HCC tumor tissues and 4 paired adjacent normal tissues, along with peripheral blood samples collected from patients with confirmed HCC diagnoses through clinical and histopathological evaluation at the Second Affiliated Hospital of Guangzhou Medical University. The research protocol received approval from the Institutional Research Ethics Committee, and written informed consent was obtained from all participants prior to sample collection. All specimens were stored under standardized biobanking conditions and exclusively utilized for research purposes in accordance with ethical guidelines.

Detection of YEATS2 concentration in serum

Peripheral blood was collected by venipuncture, and serum was obtained through centrifugation (3,000 rpm, 15 min, 4 °C) before storage at −20 °C. Serum YEATS2 levels were quantified using a commercial ELISA kit (#AE10944HU, Wuhan Abebio Science, China). Standards (0–10 ng/ml) and samples were added to pre-coated 96-well plates, incubated (1 h, 37 °C), then treated with HRP-conjugated antibody (30 min, 37 °C) after washing. Following TMB substrate (100 μL) incubation (15 min, dark) and reaction termination (50 μL stop solution), absorbance was measured at 450 nm (BioTek Synergy HT, USA). A standard curve was constructed in Excel using blank-corrected OD values, with 4-parameter logistic regression for optimal fitting (*R*² > 0.90). Sample concentrations were calculated from the curve, exceeding 5 ng/ml were reanalyzed after appropriate dilution to ensure measurements fell within the linear range (0.31–5 ng/ml).

Immunohistochemistry (IHC)

Clinical samples¹⁶ were processed through fixation, paraffin-embedding, sectioning, and deparaffinization. After antigen retrieval and blocking, sections were incubated with anti-YEATS2 antibody (#ab254895, Abcam, USA), then stained with 3,3'-Diaminobenzidine and hematoxylin. Two blinded observers scored staining intensity (1: none; 2: weak; 3: moderate; 4: strong) and proportion of positive tumor cells (0: 0%; 1: <10%; 2: 10–35%; 3: 35–75%; 4: >75%). The staining index (SI) was calculated by multiplying intensity and proportion scores. Samples with SI ≥ 8 were classified as high expression, while SI < 8 indicated low expression.

Cell culture and stable cell line establishment

Nine human HCC cell lines (MHCC97H, QGY-7701, HCCC-9810, QGY-7703, HepG2, SMMC-7721, HCCLM3, Huh7, Hep3B) were obtained from Guangzhou IGE Biotechnology (China) and cryopreserved at the Central Laboratory of the Second Affiliated Hospital of Guangzhou Medical University. Normal human hepatocytes (MIHA, #YS4004C) were acquired from Shanghai YaJi Biological (China). All cell lines were cultured under standard conditions (37 °C, 5% CO₂). HCC cells were maintained in DMEM (#12491023, Thermo Fisher Scientific, USA) with 10% FBS (#10099158, Thermo Fisher Scientific, USA), while MIHA cells were grown in RPMI-1640 medium (#12633020, Thermo Fisher Scientific, USA) supplemented with 10% FBS. For functional studies, full-length human YEATS2 cDNA was PCR-amplified and cloned into pcDNA3.1 vector (Guangzhou IGE Biotechnology, China). Stable overexpression was achieved via retroviral transduction using HEK293T packaging cells, followed by puromycin selection (0.5 μg/mL, #A1113803, Thermo Fisher Scientific, USA) for 10 days. Polyclonal populations were verified by Western blot before experimental use.

Western blot analysis

Tissues/cells were lysed in RIPA buffer supplemented with protease inhibitors. Protein samples (30 μg) were separated by 10% SDS-PAGE and transferred to PVDF membranes (300 mA, 90 min). After blocking with 5% non-fat milk for 1 h, membranes were incubated overnight at 4 °C with primary antibodies against YEATS2 and GAPDH (#AF9233/#AF7021, Affinity Biosciences, USA), E-cadherin and Vimentin (#3195/#5741, Cell Signaling Technology, USA). HRP-conjugated secondary antibodies were then applied for 1 h, followed by ECL

detection using a ChemiDoc system. GAPDH was reprobed after stripping. All other reagents were obtained from the Western Blot Kit (#WK001, Guangzhou Biolight Biotechnology, China).

Cell proliferation assay

HCCLM3 cells were seeded in 6-well plates at 1×10^3 cells/well and cultured for 10 days in DMEM with 10% FBS, with medium refreshed every 3 days. Colonies were fixed with 4% paraformaldehyde for 15 min, stained with 0.1% crystal violet for 30 min, and rinsed with PBS. Visible colonies (≥ 50 cells/colony) were quantified using ImageJ software (v1.53) under an inverted microscope (Olympus, Japan). Triplicate wells were analyzed per group, and data normalized to control conditions.

Wound healing assay

HCCLM3 cells were seeded uniformly at 2×10^4 cells/well in 6-well plates (#CLS3335, Corning, USA) and cultured in DMEM with 10% FBS until 90% confluency (24 h). After serum starvation (0.5% FBS, 24 h), three parallel scratches per well were generated using a sterile 100 μ L pipette tip (diameter 0.6 mm). Debris was removed by PBS washes (3 times). Cells were then incubated in complete medium (10% FBS) under 5% CO₂ at 37°C. Migration progression was documented at 0/12/24 h using an inverted phase-contrast microscope (Olympus, 20 \times objective) with a calibrated grid. Wound closure rates (%) were quantified via ImageJ (v1.53) using the “MRI Wound Healing Tool” plugin. Triplicate experiments were normalized to baseline (0 h).

Transwell Invasion Assay

HCCLM3 cells (2×10^4 cells/well in 200 μ L serum-free DMEM) were seeded into Matrigel-coated (#CLS354234, Corning, USA) Transwell inserts (#CLS3460, Corning, USA). The lower chamber contained DMEM with 10% FBS as a chemoattractant. After 36 h incubation (37°C, 5% CO₂), non-invaded cells were removed by cotton swab. Invaded cells were fixed with 4% paraformaldehyde (30 min), stained with 0.5% hematoxylin (10 min), and imaged under an inverted microscope (Olympus, 20 \times). Five random fields per insert were counted using Image J 1.35.

3D spheroid invasion assay

HCCLM3 cells (1×10^4 cells/well) were trypsinized, resuspended in DMEM/F12 medium (#21331046, Thermo Fisher Scientific, USA) containing 5% FBS, and mixed with Growth Factor Reduced Matrigel (2%, #CLS356231, Corning, USA). The cell-Matrigel suspension (500 μ L/well) was plated in pre-chilled 24-well plates (#CLS3473, Corning, USA) and polymerized at 37°C for 30 min. Cultures were maintained with 2% Matrigel-supplemented medium, which was carefully replaced every 48 h using pre-cooled pipettes. Spheroid formation and invasion were monitored every 48 h for 10 days using phase contrast microscopy (Nikon, 20 \times). Five random fields per well were imaged, and invasion area was quantified using ImageJ (v1.53) with the “3D Sphere Analyzer” plugin.

Immunofluorescence analysis

Transfected HCCLM3 cells (5×10^4 cells/well) were plated in poly-L-lysine-coated 6-well plates (#CLS356515, Corning, USA). After 24 h, cells were fixed with 4% paraformaldehyde, permeabilized with 0.2% Triton X-100, and blocked with 5% BSA. Primary antibodies against E-cadherin (1:200, #20874-1-AP, Proteintech, USA) and Vimentin (1:150, #10366-1-AP, Proteintech, USA) were applied overnight at 4°C, followed by Rhodamine Red-X-conjugated secondary antibodies (1:200, 1 h) (1:200, 115-025-003, Jackson ImmunoResearch, USA). Nuclei were stained with DAPI (1 μ g/mL, 10 min, dark), mounted with ProLong Gold, and imaged via Olympus FV1000 confocal microscope (60 \times , 0.5 μ m Z-stacks). Images were analyzed using ImageJ (v1.53) post-background subtraction.

Comprehensive analysis and enrichment analysis of Protein-Protein interactions (PPI)

Search Tool for the Retrieval of Interacting Genes/Proteins (STRING) (<https://cn.string-db.org/>)¹⁷ and Cytoscape¹⁸ were used for network analysis of the YEATS2 gene, setting the analysis for 50 interacting molecules with a minimum interaction score of 0.7. Networks were constructed using Cytoscape, and hub genes were identified using plugins. Nodes were evaluated using degree, Maximum Neighborhood Component (MNC), Maximum Clique Centrality (MCC), Edge Percolation Component (EPC), stress, and closeness metrics, selecting the top 10 nodes. Single-gene enrichment analysis for Gene Ontology (GO), Kyoto Encyclopedia of Genes and Genomes (KEGG)¹⁹, and Hallmark pathways was conducted using BEST. Enrichment Analysis results were evaluated based on Normalized Enrichment Score (NES) and *P*-values. Gene sets with False Discovery Rate (FDR) < 0.25 and adjusted *P* < 0.05 were considered significantly enriched.

MTT drug resistance assay

Logarithmically growing cells were collected and suspended. 100 μ L of this suspension was pipetted into each well of a 96-well flat-bottom plate (#267544, Thermo Fisher Scientific, USA), yielding a cell density of 1×10^3 – 10^4 cells/well. Peripheral wells were filled with PBS to prevent evaporation. The plate was incubated at 37°C under 5% CO₂ until HCCLM3 cells formed a confluent monolayer. Then, 200 μ L diluted drug solutions (Cisplatin, 0.25–40 mg/L, #15663-27-1, Abmole Bioscience, USA; Sorafenib, 0.5–32 μ mol/L, #284461-73-0, Abmole Bioscience, USA) were added per well. After 5 days of incubation, 20 μ L methylthiazolyl diphenyl-tetrazolium bromide (MTT, #298-93-1, Abmole Bioscience, USA) solution was added, and incubation continued for 4 h. The culture medium was aspirated, replaced with 150 μ L DMSO (#67-68-5, Abmole Bioscience, USA), and shaken gently for 10 min to dissolve formazan crystals. Absorbance at 490 nm was then measured for each well.

Evaluation of therapeutic benefits in clinical patients

HCC patients undergoing transcatheter arterial chemoembolization (TACE) or anti-PD-L1 treatment were categorized into significant (score ≥ 60) and non-significant (score < 60) efficacy groups, using a weighted scoring system (Supplementary Table S2). Serum YEATS2 levels were subsequently quantified in both groups.

Statistical analysis and ethics approval

All in vivo experiments were performed in triplicate. Statistical analyses were conducted using GraphPad Prism 6, with the χ^2 test being applied for categorical data comparisons (e.g., incidence rates) and Student's t-test being used for continuous variable analyses (e.g., fluorescence intensity, invasion area). Significance was set at $P < 0.05$. Human participant blood samples were utilized exclusively with the informed consent of the individuals and their legal guardians. The study was approved by the Ethics Committee of The Second Affiliated Hospital of Guangzhou Medical University. All experiments were performed in accordance with relevant guidelines and regulations.

Result

Acetylation gene YEATS2 as a diagnostic marker for HCC

Among the 99 differentially DEGs screened (Supplementary Table S3), 11 were upregulated and one was downregulated (Fig. 1A). Lasso regression (Fig. 1B, Supplementary Table S4) and Univariate Cox analysis (Fig. 1C) identified YEATS2 as the strongest associated with RFS of HCC patients. Various HCC datasets demonstrated increased YEATS2 expression in tissues (Fig. 1D). ROC analysis showed higher sensitivity and specificity for YEATS2 compared to AFP in TCGA (Fig. 1E). YEATS2 protein levels were elevated in cancerous tissues and serum of HCC patients from our cohort (Figs. 1F–H).

YEATS2 as a promising biomarker for HCC

Clinical data from TCGA patients showed variations in YEATS2 expression across different age groups, tumor statuses, pathologic T stages, pathologic stages, histologic grades, and alpha-fetoProtein (AFP) levels (Supplementary Table S5). Notably, multiple clinical studies have justified an age stratification at 65 years, effectively discriminating disease progression patterns in HCC^{20,21}. Intriguingly, TCGA analysis revealed higher YEATS2 expression in younger patients (≤ 65 years) compared to older patients (Fig. 2A), although grouped comparisons across different ages showed no significant differences ($P > 0.05$) in TCGA and other cohorts (Fig. 2B). This trend of higher YEATS2 expression in younger patients was consistently observed across various datasets, hinting at potential mechanisms such as age-related decline in DNA repair efficiency impacting the accumulation of epigenetic changes recognized by YEATS2 (e.g., H3K27ac/H3K9ac)⁶, or alterations in lipid metabolism and epigenetic regulator expression in aging hepatocytes²². Such insights may provide valuable considerations for the clinical application of YEATS2. Furthermore, statistically significant differences ($P < 0.05$) in YEATS2 expression were observed between different pathologic T stages (Fig. 2C), pathologic stages (Figs. 2D, E), tumor statuses (Fig. 2F), histologic grades (Fig. 2G), and AFP levels (Figs. 2H, I) across both TCGA and other datasets. Moreover, YEATS2 expression was not influenced by smoking status (Figure S1A), hepatitis virus infection (Figures S1B–D), or liver multinodularity (Figure S1E). All the GSE datasets other than TCGA-LIHC and the analysis results are directly derived from the BEST database.

High YEATS2 expression predicts poor prognosis in HCC

Cox regression analysis was performed across multiple HCC-related datasets, including TCGA, GSE54236, GSE114269, GSE14520, GSE116174, ICGC, TABM, GSE271550, and GSE76427, to assess the impact of YEATS2 expression on overall survival (OS), disease-specific survival (DSS), disease free survival (DFS), recurrence-free survival (RFS), and progression-free survival (PFS) (Fig. 3A). Statistically significant associations were further validated using log-rank tests (Figs. 3B–G). The results consistently suggested that upregulation of YEATS2 serves as a risk factor for accelerated mortality in HCC patients.

Time-dependent ROC analysis of the TCGA-HCC cohort revealed that the area under the curve (AUC) values for OS, DSS, and PFS were all above 0.5 at various time points (Figs. 3H–J), indicating the predictive power of YEATS2 expression in these survival metrics. The consistency of results across diverse datasets and statistical methods underscores that high YEATS2 expression is a reliable indicator of poor prognosis in HCC.

Gene Set Enrichment Analysis (GSEA) conducted on various TCGA sub-datasets revealed a negative correlation between YEATS2 expression and tumor survival (Figs. 3K, L), as well as a positive correlation with recurrence (Figs. 3M–P). These findings provide further evidence supporting the role of YEATS2 as a prognostic biomarker in HCC.

YEATS2 promotes tumorigenicity of HCC cells in vitro

Our study observed elevated YEATS2 expression in nine hepatocyte-derived cancer cells (Fig. 4A), albeit with discrepancies in Western blot results compared to published data (Huh7/HepG2)¹¹, potentially attributed to technical factors such as antibody sources, internal controls, batch-specific epitope recognition, cell line variations, and methodological differences in sample preparation and detection parameters²³, particularly for post-translationally modified YEATS2 isoforms. To investigate YEATS2's role in HCC, we employed an overexpression strategy for three reasons: it directly demonstrates oncogenic functions by affecting HCC cell proliferation, migration, invasion, and EMT; mimics clinical pathology as YEATS2 overexpression is common in HCC patients; and complements previous gene silencing studies for a comprehensive understanding¹¹. For validation, we selected the highly metastatic HCCLM3 cell line (Supplementary document-1), suitable for studying YEATS2's role in cancer metastasis due to its aggressive phenotype aligned with advanced HCC progression (Fig. 4B).

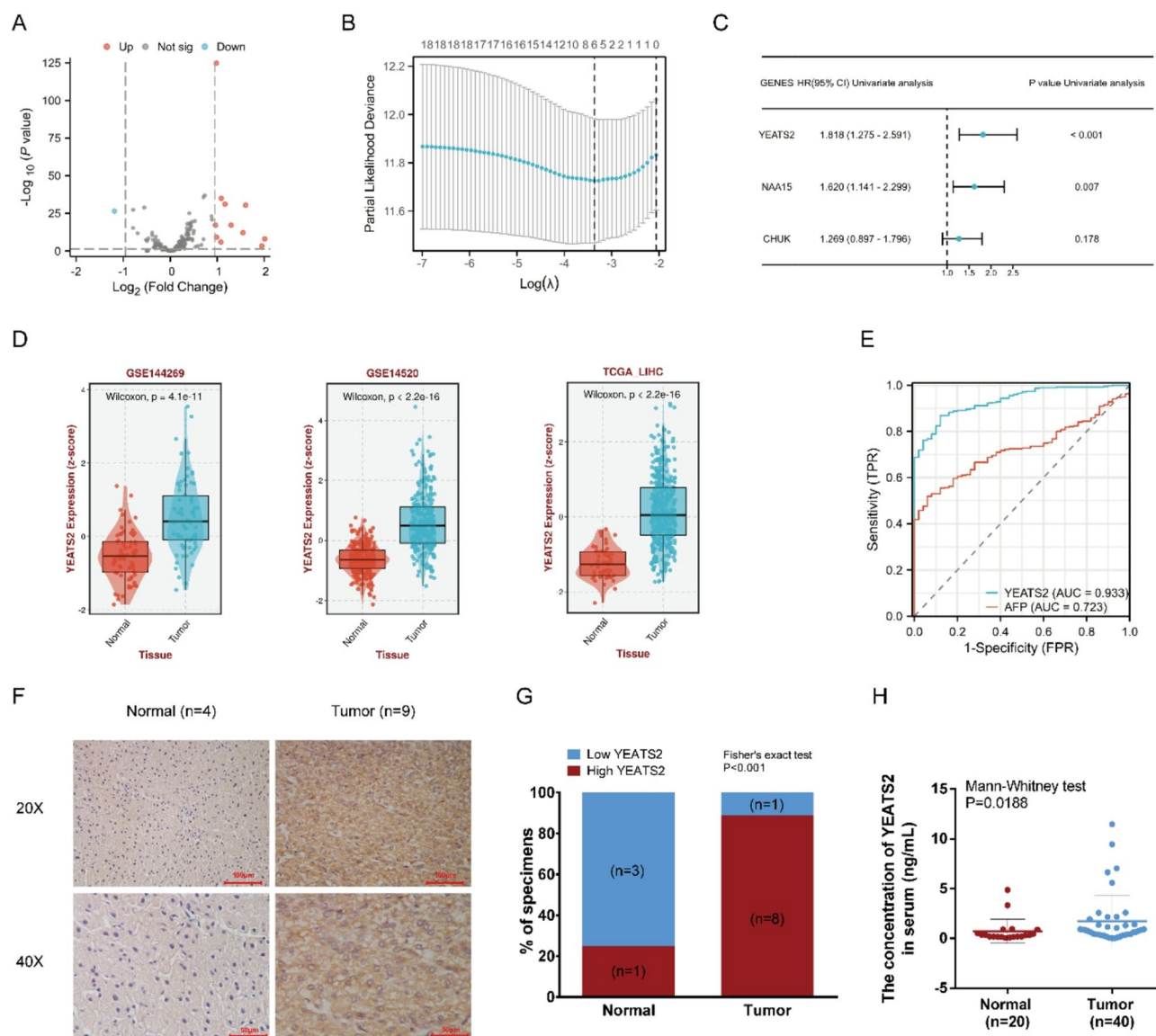


Fig. 1. Acetylation-Related Gene YEATS2 is Upregulated in HCC. (A) Expression differences of 240 acetylation-related genes in HCC from the TCGA database. (B) LASSO analysis of DEGs. (C) Cox analysis results of target genes on RFS in HCC patients. (D) Relative expression levels of YEATS2 from various databases. (E) ROC curve analysis of YEATS2 and AFP in HCC from TCGA. (F, G, H) Elevated YEATS2 Levels in tissues and serum of HCC Patients. Statistical analyses were conducted using GraphPad Prism 6.

Results showed increased invasion in Transwell assays (Fig. 4C), enhanced migration in wound healing (Figs. 4D), enhanced colony formation (Figs. 4E), and aggressive invasion in 3D spheroid assays (Fig. 4F), suggesting that YEATS2 promotes HCC cell proliferation, migration, and invasion. Similar results also apply to the in vitro study of HepG2 cells (Figure S2). Additionally, YEATS2 upregulation of Vimentin and downregulation of E-cadherin (Figs. 4G, H) confirmed EMT, facilitating cancer dissemination, invasion, and therapeutic resistance²⁴.

YEATS2 protein interactions and functional enrichment analysis

PPI network analysis identified WDR5 as the strongest hub among interacting partners including MOCS2, CCDC101, TADA2A, TADA3, CSRP2BP, KAT2A, KAT2B, MBIP, and TADA2B (Fig. 5A). WD repeat-containing protein 5 (WDR5), a core component of histone methyltransferase complexes, enhances histone H3 lysine 4 trimethylation (H3K4me3)²⁵ that drives HCC invasion and proliferation²⁶. GSEA across GO, KEGG, and Hallmark databases (Figs. 5B-D) linked elevated YEATS2 expression to enhanced mitotic DNA replication, spliceosome function, and cell cycle progression (specifically E2F targets and G2M checkpoint), suggesting YEATS2 promotes HCC proliferation through cell cycle regulation^{27,28}. Conversely, negative correlations focused on fatty acid and xenobiotic metabolism. Restricted fatty acid availability impedes cancer dissemination²⁹, while impaired xenobiotic metabolism promotes necrotic inflammation and mitochondrial dysfunction, elevating

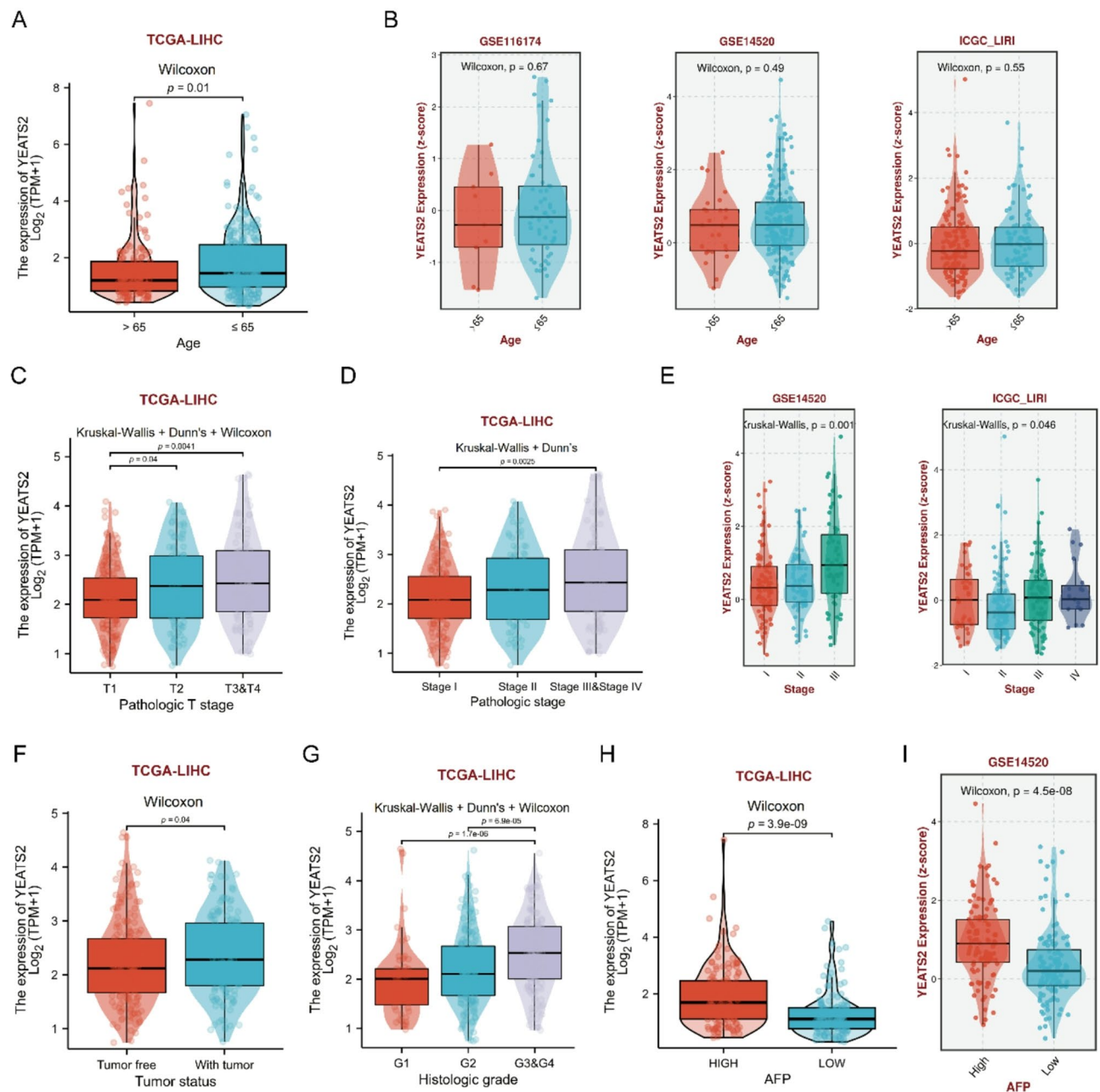


Fig. 2. YEATS2 Expression Analysis in HCC Patient Cohorts. (A, B) Differential YEATS2 expression across age groups in TCGA and HCC datasets. (C–E) YEATS2 expression analysis stratified by disease stages in TCGA and HCC datasets. (F) Expression variations in tumor status. (G) Expression changes across histologic grades. (H, I) Differential analysis of YEATS2 across AFP levels in two HCC datasets.

reactive oxygen species (ROS) that activate Kupffer and stellate cells to drive inflammation and fibrosis³⁰. Elevated YEATS2 thus facilitates HCC progression by suppressing these protective metabolic pathways.

Synthesizing these findings³¹, YEATS2 may regulate HCC through three interconnected mechanisms: (1) Promoting G1/S transition and G2/M progression via chromatin remodeling-mediated upregulation of E2F targets and checkpoint genes, amplified through WDR5 interaction at proliferative gene promoters. (2) Orchestrating metabolic reprogramming to inhibit fatty acid oxidation and redirect lipids for biosynthesis, while impairing xenobiotic detoxification. (3) Activation of the inflammation-fibrosis axis established a pathogenic feedforward loop that drives HCC aggression.

YEATS2 and immune infiltrates in HCC

Tumor-infiltrating immune cells play pivotal roles in HCC progression through dynamic regulation of inflammatory networks. Our multi-omics analysis (Fig. 6A) across eight independent cohorts (TCGA/GEO) employing eight computational algorithms (CIBERSORT, EPIC, etc.; concordant results from ≥ 2 methods

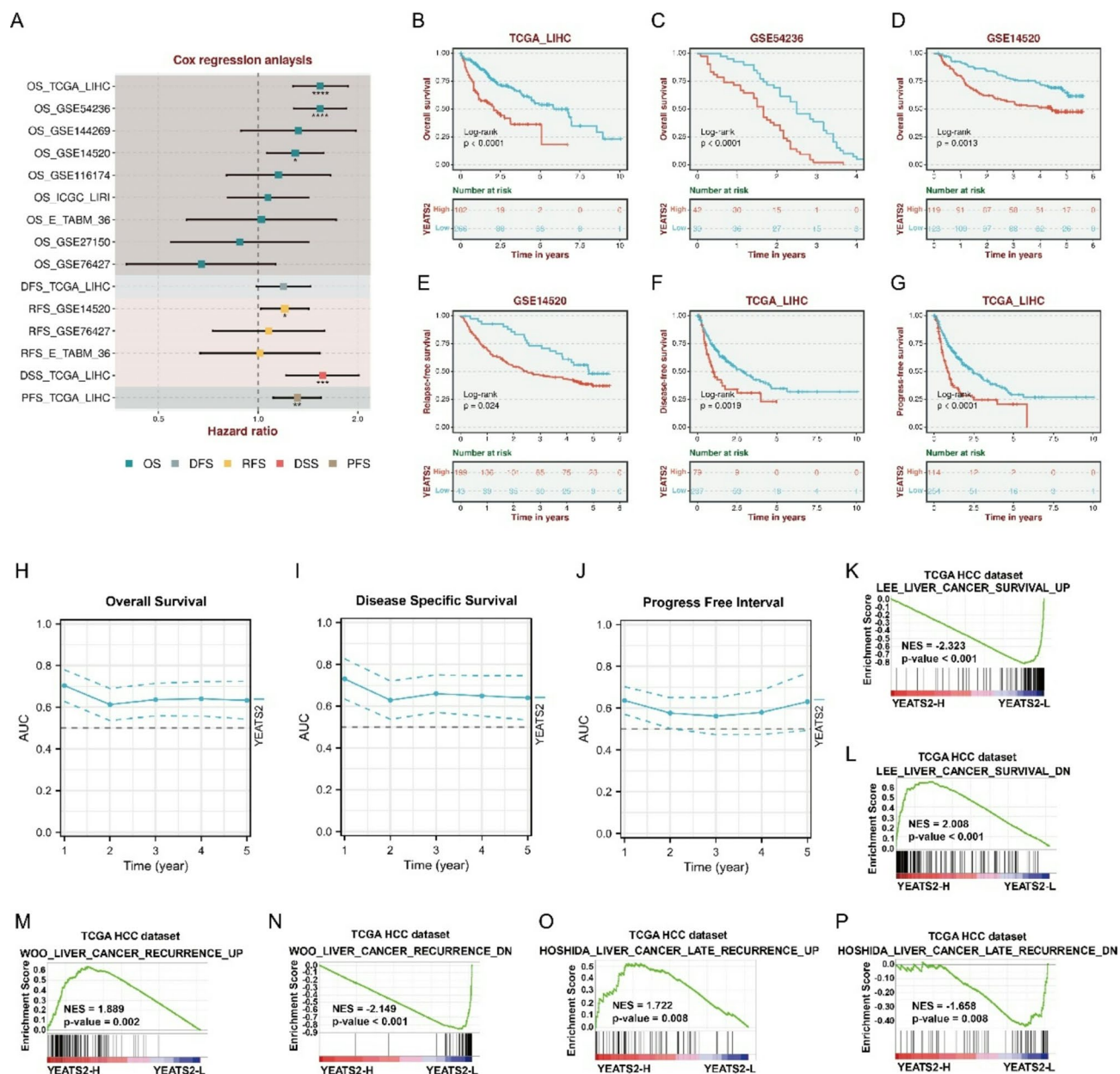


Fig. 3. YEATS2's Impact on HCC Patient Survival. **(A)** Cox regression analysis across multiple datasets assessing YEATS2's role. **(B–G)** YEATS2 expression's effect on survival time in various datasets. **(H–J)** Time-dependent ROC analysis of YEATS2 in HCC-TCGA. **(K–P)** GSEA reveals YEATS2's significant association with survival and recurrence-related gene signatures in TCGA mRNA datasets.

required) demonstrates that elevated YEATS2 expression consistently promotes monocyte recruitment (Figs. 6B–J) while suppressing mast cell and NK cell infiltration (Figs. 6K–V).

Monocyte-derived tumor-associated macrophages (TAMs) drive HCC progression via vascular endothelial growth factor (VEGF)-mediated angiogenesis, immunosuppressive cytokine release, and metastasis facilitation³². Conversely, NK cells - the primary antitumor effectors - mediate tumoricidal activity, antiviral defense, and HBV-specific hepatocyte clearance³³. Interestingly, YEATS2 knockdown in xenograft models reduced tumor growth while increasing senescent cells and intratumoral NK cell accumulation¹¹, corroborating the observed YEATS2-NK cell inverse correlation that may underlie its age-dependent expression patterns as mentioned above. Mast cells show context-dependent roles: while tumor-promoting through cytokine secretion³⁴, their matrix-remodeling capacity can paradoxically limit HCC dissemination³⁵.

Impact of YEATS2 on HCC treatment

Early HCC is treatable surgically, but approximately 20% of patients present with microvascular invasion (MVI), correlating with poor prognosis. While sorafenib remains the sole approved first-line systemic therapy, its

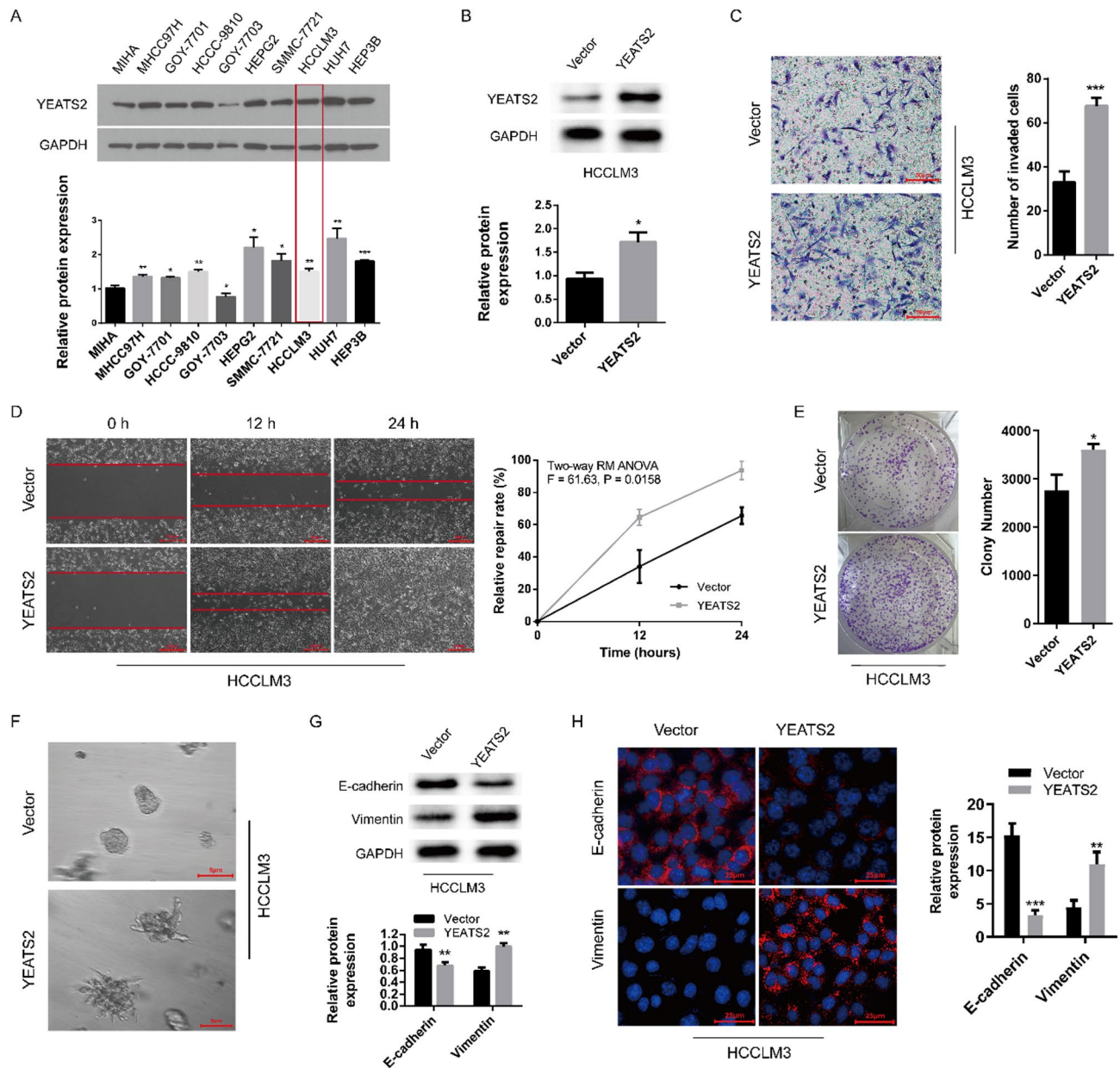


Fig. 4. YEATS2 Enhances HCC Cell Proliferation, Migration, and Invasion. **(A)** Western blot analysis of YEATS2 overexpression, the grouping of blots cropped from the same gel. **(B)** The outcome of YEATS2 overexpression, the grouping of blots cropped from different parts of different gels under the same experimental conditions. **(C)** Transwell assay showed invasiveness of YEATS2-overexpressing cells. **(D)** Wound-healing assay revealed motility differences. **(E)** Colony growth comparison of YEATS2-overexpressing cells. **(F)** 3D spheroid invasion assay of YEATS2-modulated cells. **(G)** YEATS2 overexpression altered E-cadherin and Vimentin levels, the grouping of blots cropped from different gels under the same experimental conditions. **(H)** Expression and localization of E-cadherin/Vimentin upon YEATS2 modulation. Error bars indicate mean \pm SD (*, $P < 0.05$. **, $P < 0.01$. ***, $P < 0.001$).

efficacy is limited and MVI further diminishes treatment response. Recent advances demonstrate promising outcomes with locoregional therapies like TACE and radiotherapy in advanced HCC with MVI, particularly when combined with sorafenib³⁶.

Integrated analysis of drug sensitivity correlations (GDSC1/2 and CTRP datasets) and expression profiling (TCGA-LIHC, GSE116174/104580/109211) revealed that elevated YEATS2 expression may modulate therapeutic responses in HCC, inducing drug resistance while minimally affecting radiotherapy and MVI status. Cross-database analyses indicate that high YEATS2 expression increased resistance to Selumetinib, Etomoxir, Hyperforin, and Tamoxifen but conferred sensitivity to platinum-based agents (cisplatin/carboplatin) and statins (Figs. 7A, C, D)³⁷. In vitro cisplatin resistance assays confirmed dose-dependent reductions in viability (0–40 mg/L), with repeated-measures ANOVA revealing significant differences between YEATS2-overexpressing

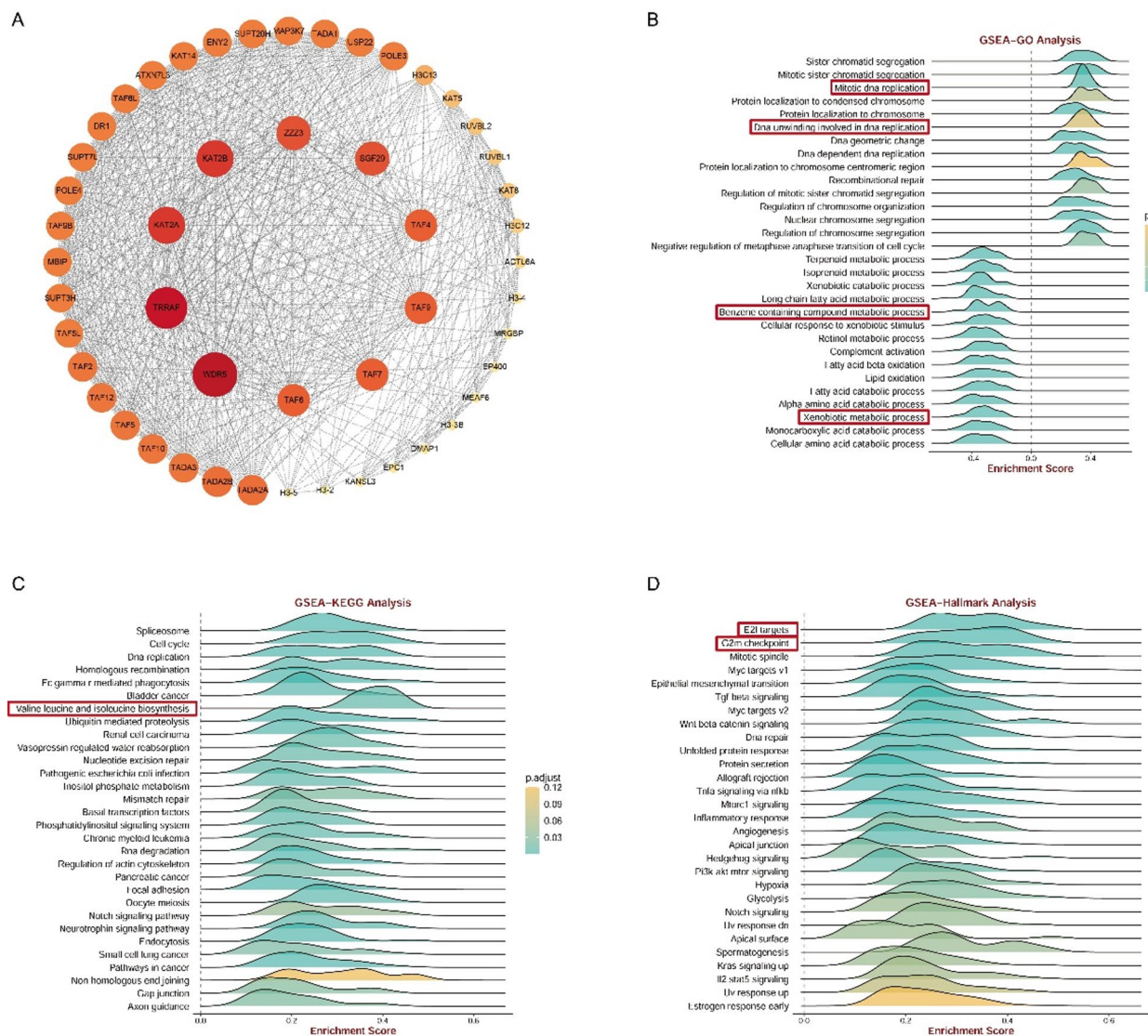


Fig. 5. YEATS2-Interacting Proteins and Functional Enrichment in HCC. (A) Annotation of YEATS2-interacting proteins and their co-expression patterns. **(B-D)** Functional enrichment analysis results from GSEA.

and control groups (Fig. 7B). Pronounced resistance divergence occurred at low cisplatin concentrations (<3 mg/L), while attenuated differences at higher concentrations (>10 mg/L) suggest YEATS2-mediated resistance may be masked by overwhelming cytotoxicity. Elevated YEATS2 also correlated with diminished response to TACE and sorafenib (Figs. 7G, I), though clinical data showed no association between serum YEATS2 and TACE efficacy (Fig. 7H). YEATS2 overexpression consistently enhanced sorafenib resistance in HCC cells, exhibiting distinct concentration dependence: negligible differences at ≤ 4 $\mu\text{mol/L}$ versus significant disparities at >8 $\mu\text{mol/L}$ (Fig. 7J).

Critically, analyses of TCGA and GSE116174 datasets revealed no significant association between YEATS2 expression and either radiotherapy outcomes or postoperative MVI status (Figs. 7E, F), indicating minimal involvement in radiation-induced DNA repair or vascular invasion mechanisms³⁵. These findings underscore YEATS2's central role in chemoresistance pathways, warranting expanded clinical validation.

YEATS2 interactions on HCC immunotherapy

Immune checkpoint (IC)-based immunotherapy has emerged as a transformative approach in HCC, leveraging co-inhibitory/co-stimulatory signals to selectively target tumor cells while preserving healthy tissues³⁸. ROC analysis indicates YEATS2 expression may predict immunotherapy response (AUC>0.5, Figs. 8A-G), with elevated levels observed in anti-PD-L1 (programmed death-ligand 1)-responsive HCC patients (Figs. 8H-N).

Notably, among HCC patients undergoing anti-PD-L1 immunotherapy, those with elevated YEATS2 expression exhibited superior survival outcomes compared to their low-expression counterparts (Figs. 80-U). This comprehensive analysis emphasizes YEATS2's heightened sensitivity to anti-PD-L1 in HCC with

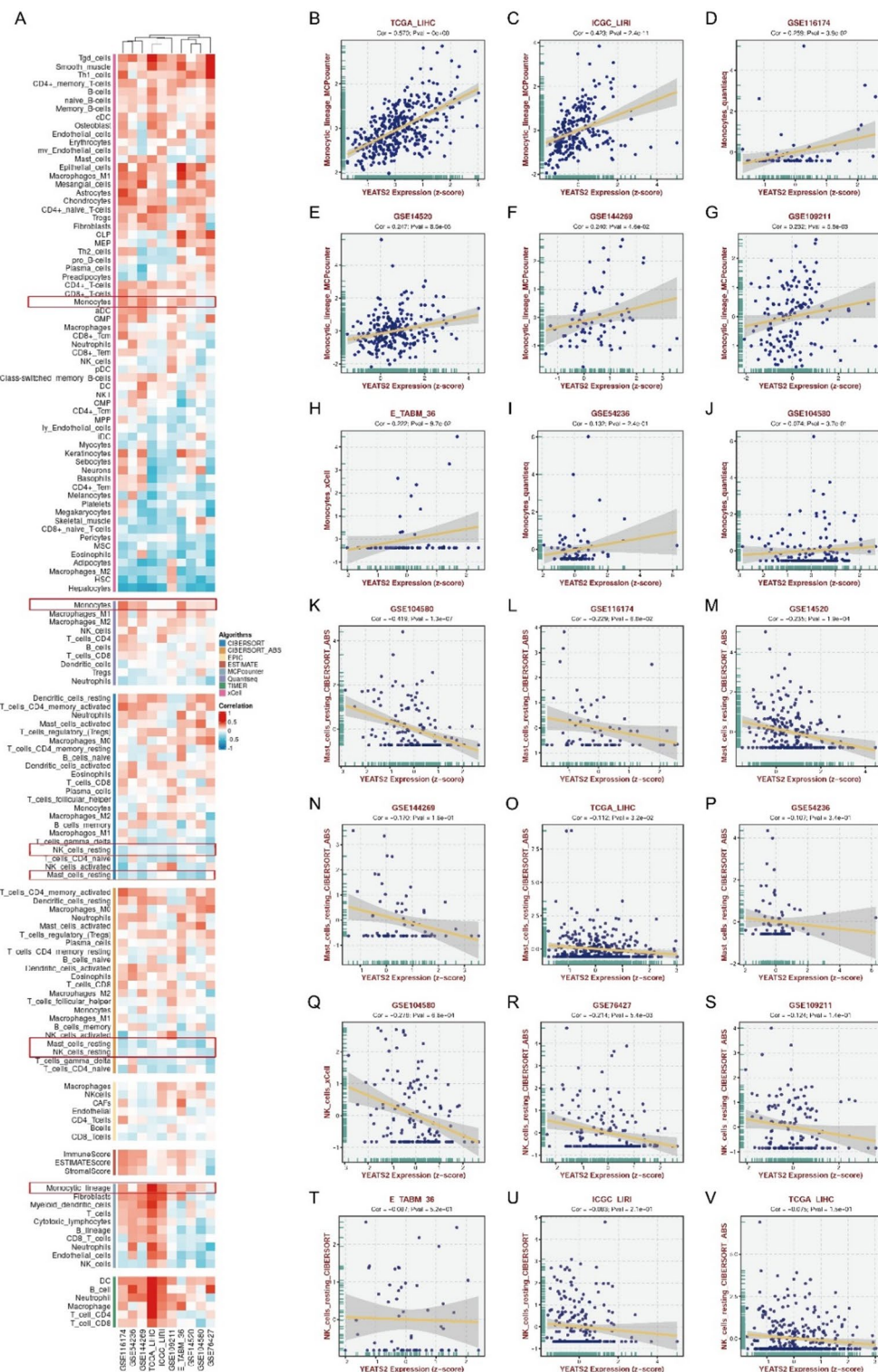


Fig. 6. YEATS2 Correlation with Immune Infiltrates in HCC. (A) Immune cell infiltration analysis of YEATS2 in HCC, with red boxes indicating positive correlations and green boxes indicating negative correlations. (B–J) Positive correlation of YEATS2 with monocytes across multiple datasets. (K–P) Negative correlation of YEATS2 with mast cells in various HCC datasets. (Q–V) Negative correlation of YEATS2 with NK cells across multiple datasets.

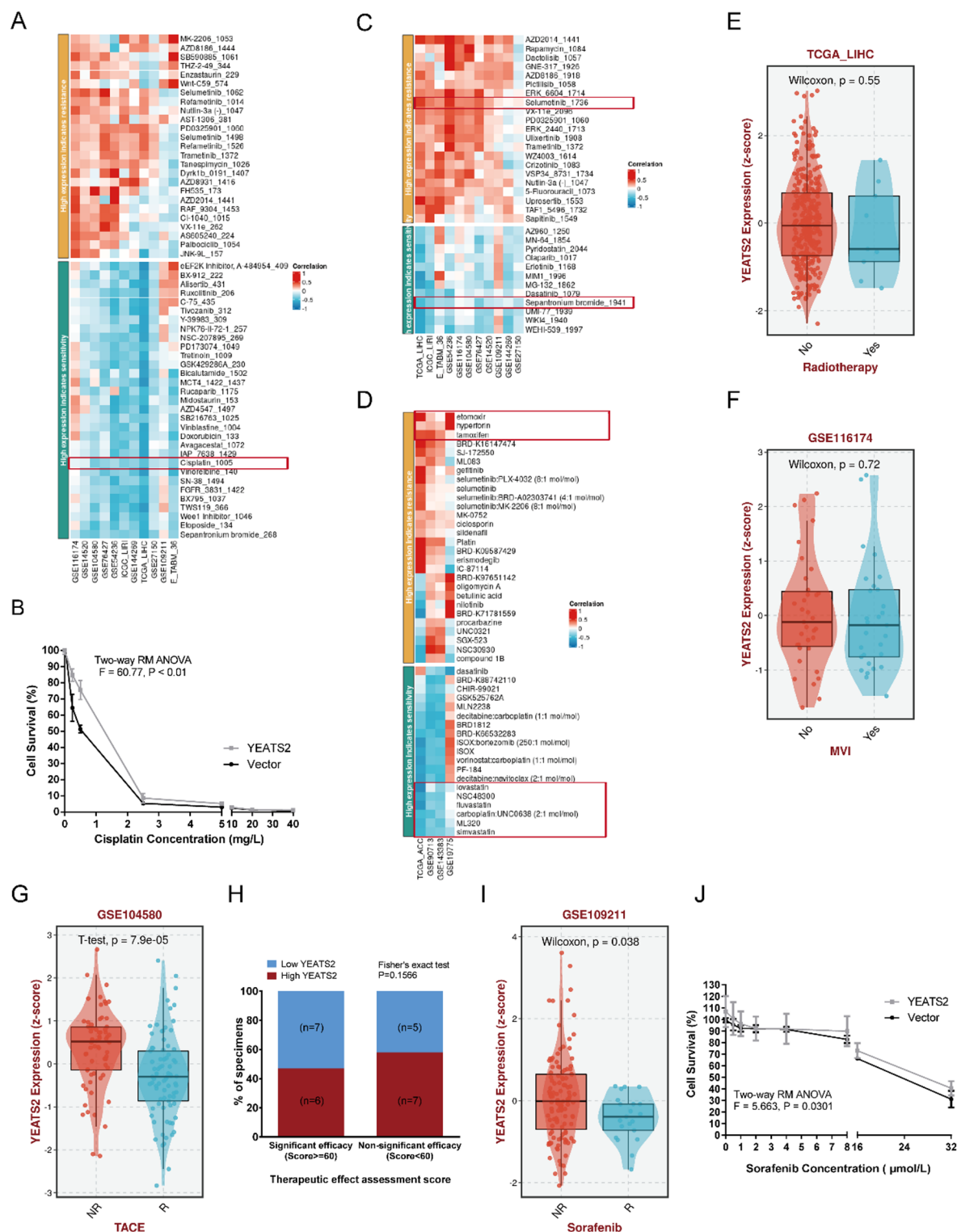


Fig. 7. Impact of YEATS2 on Various HCC Treatments. **(A)** Evaluate the impact of YEATS2 on sensitivity to chemotherapy drugs in liver cancer via GDSC1 analysis. **(B)** MTT assay to assess cisplatin resistance. **(B, C)** Analyze the influence of YEATS2 on HCC chemosensitivity using GDSC2 and CTRP datasets, respectively. **(E–F)** Explore YEATS2 expression differences in varying radiotherapy outcomes and MVI presence post-surgery across diverse datasets. **(G–H)** Analyze YEATS2's effect on TACE efficacy and validate the correlation between serum YEATS2 levels and TACE response. **(I–J)** Assess YEATS2's influence on sorafenib efficacy in HCC patients, complemented by MTT assays examining YEATS2's role in HCC cell sorafenib resistance.

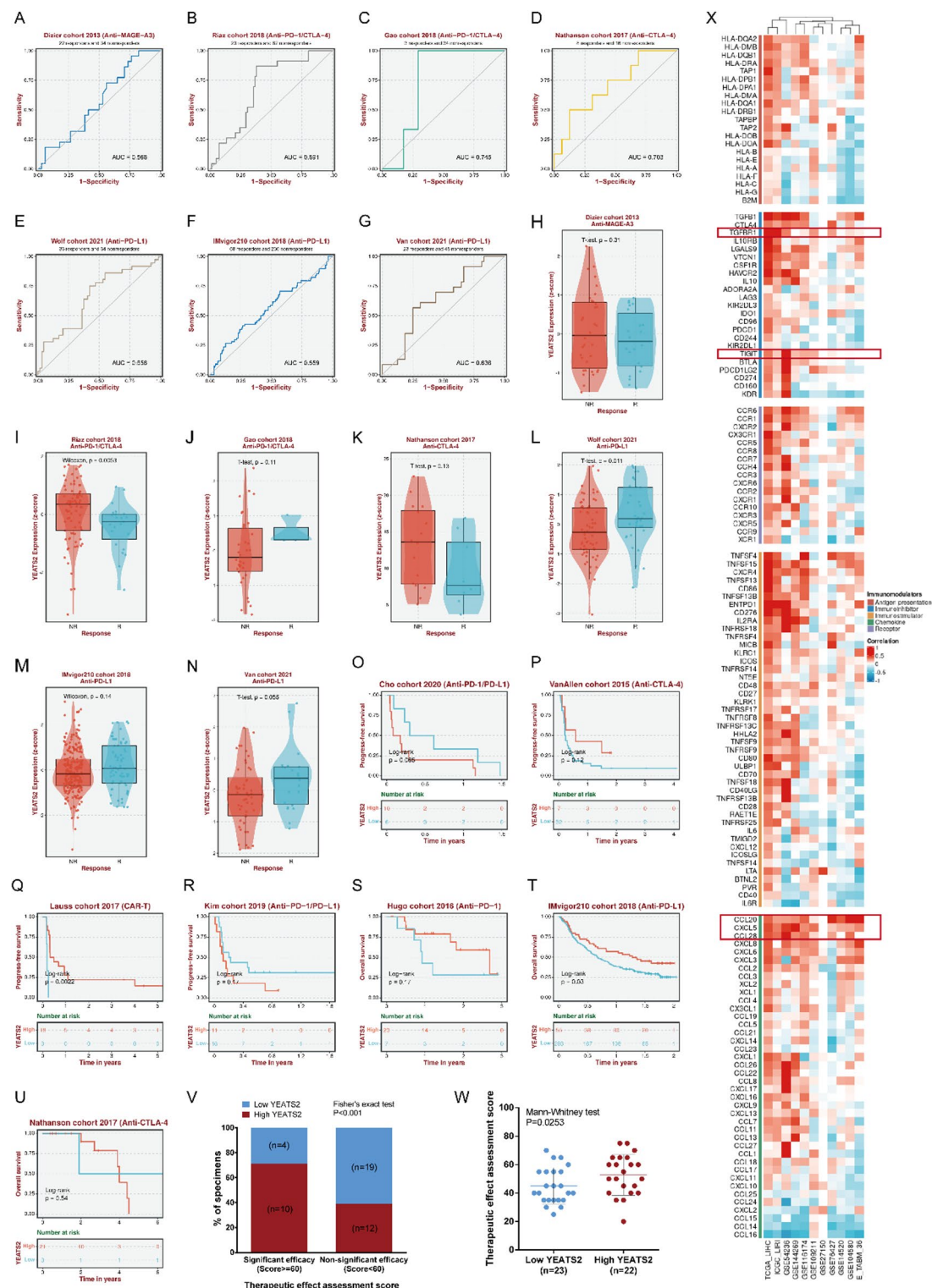


Fig. 8. YEATS2's Influence on Tumor Immune System and Immunotherapy Outcomes. (A–G) ROC curve analyses illustrate the predictive value of YEATS2 expression for various HCC immunotherapy strategies. (H–N) Comparisons of YEATS2 expression levels across immunotherapy efficacy groups. (O–U) Survival analyses reveal the impact of YEATS2 expression on HCC patients undergoing different immunotherapies. (V–W) Clinical validation of the correlation between serum YEATS2 levels and response to anti-PD-L1 therapy. (X) Correlation analysis of YEATS2 with key molecules in the tumor immune system.

overexpression, supported by our clinical validation (Figs. 8V, W). Recent studies suggest YEATS2 modulates immune evasion³⁹, particularly through PD-L1/PD-1 axis suppression of T-cell activation—a mechanism implicating YEATS2 in tumor immune escape. Multi-dataset analysis further reveals YEATS2's regulatory effects on immunosuppressive markers (TGFB1, TIGIT) and chemokines (CCL20, CXCL5, CCL28; Fig. 8X), positioning it as a multifaceted immunomodulator in HCC.

Discussion

YEATS2, a histone H3K27ac reader, epigenetically modulates vital transcriptional programs for cellular functions⁴⁰. Cancerous dysregulation or mutations in YEATS2 spur aberrant gene expression and chromatin alterations, fueling oncogenesis⁴¹. It also emerges as a therapeutic target demonstrating Huachansu's efficacy in delaying pancreatic adenocarcinoma via YEATS2/TAK1/NF- κ B inhibition⁴². Distinct from prior investigations, this study establishes novel insights into YEATS2's role in HCC. First, multi-center tissue samples and institutional serum monitoring validated concordance between tissue and circulating YEATS2 levels, providing direct evidence for noninvasive diagnostics⁹. Second, reinforcing prior findings that YEATS2 promotes HCC progression via PI3K/AKT signaling, we employed diverse cell lines for in vitro experiments integrated with single-gene GSEA and Hallmark pathway analysis, strengthening evidence that YEATS2 augments HCC proliferation through PI3K-associated mechanisms—specifically by inducing cell cycle arrest and dysregulating DNA replication¹⁰. Methodologically, stable overexpression in HCCLM3 cells provided a complementary approach to shRNA knockdown models used previously¹¹, better recapitulating endogenous high-expression states while circumventing off-target effects, corroborative 3D spheroid invasion assays further substantiated YEATS2's pro-invasive role. Crucially, this work elucidates YEATS2's dual regulatory functions in EMT and tumor immune microenvironment remodeling. It further demonstrates that YEATS2 overexpression reduces sensitivity to cisplatin and sorafenib, while serum YEATS2 levels serve as a potential biomarker for predicting anti-PD-L1 immunotherapy response. Collectively spanning fundamental mechanisms to clinical translation, these findings optimize precision diagnostics and therapeutics for HCC.

Based on our integrated analysis and existing literature, we proposed that YEATS2 fostered HCC progression through multifaceted mechanisms that impacted chemoresistance and immune evasion. On one hand, YEATS2 reduced the efficacy of therapeutics including Selumetinib (MEK1/2 inhibitor), Etomoxir (fatty acid oxidation inhibitor) effect⁴³, Hyperforin (anti-proliferative agent)⁴⁴, Tamoxifen (apoptosis regulator)^{45,46}. Selumetinib targets the Ras/Raf/MEK/ERK pathway in HCC, currently under investigation for advanced cases in combination therapies. GSEA further demonstrated YEATS2's association with MEK-dependent E2F targets. Similarly, Etomoxir suppresses tumorigenesis by inhibiting CPT1A, the rate-limiting enzyme in fatty acid β -oxidation, thereby promoting apoptosis⁴³. Intriguingly, YEATS2 expression exhibited an inverse correlation with fatty acid β -oxidation activity. Given the mechanistic overlap between YEATS2 and these two drugs, competitive antagonism may arise—a hypothesis supported by GDSC2 and CTRP analyses, which revealed increased drug resistance in YEATS2-high HCC cells, aligning with metabolic dependencies in epigenetically dysregulated tumors. On the other hand, statins attenuated hepatic inflammation via GTPase prenylation inhibition and suppressed angiogenesis⁴⁷, by blocking the TBK1-IRF3-IL33 axis⁴⁸, with YEATS2 overexpression potentially enhancing these benefits. Previous studies indicated that YEATS2 drove HCC progression through enrichment of DNA repair and proliferation-related genes like E2F targets, aligning with the anti-cancer mechanism of platinum-based drugs. Analysis of the GDSC1 and CTRP databases respectively indicated that elevated YEATS2 expression correlated with increased sensitivity of HCC to cisplatin and carboplatin. However, these bioinformatics predictions contradicted our in vitro experimental results. Since the HCCLM3 cell line used in our study was not represented in either database, the discrepancy likely stems from variations in cell models, drug preparations, or treatment concentrations. The observed inconsistency therefore does not necessarily reflect methodological flaws in either approach. This unexpected divergence warrants further investigation into platinum resistance mechanisms. Future work will focus on developing cisplatin-resistant HCC cell lines and corresponding animal models to clarify YEATS2's therapeutic function and clinical relevance. In the field of tumor immunology, PPI analysis identified WDR5 as its primary binding partner, where YEATS2 cooperatively maintained H3K4 modifications at the IGF-1 enhancer with WDR5, supporting the established HBx-WDR5-IGF-1 axis that promoted immunosuppressive Treg expansion and IL-10 secretion⁴⁹. Through indirect IGF-1 regulation, YEATS2 contributed to epigenetic reprogramming and immune evasion in HCC.

YEATS2 epigenetically reshaped the tumor immune landscape by elevating monocyte infiltration while suppressing NK and mast cells. It recruited monocytes through H3K18la recognition, enhancing transcription of chemoattractants CCL2/CCL5 via competitive histone acetylation reader binding. Concurrent metabolic reprogramming suppressed fatty acid oxidation genes (CPT1A/ACADL), increasing tumor lactate secretion. Lactate accumulation promoted H3K18 lactylation, activating METTL3 to drive monocyte differentiation into immunosuppressive TAMs^{50,51}. These TAMs secreted VEGF activating VEGFR2-PI3K/AKT angiogenesis, IL-10, TGF- β , and PD-L1 inhibiting CD8+ T cells and expanding Tregs¹². They also enhanced invasion via MMP-2/9-mediated ECM degradation and EMT signaling. Conversely, YEATS2 suppressed NK cell infiltration and cytotoxicity by inhibiting NKG2D ligands (MICA/B)⁵² and DNAM-1 ligand (CD155) via enhanced H3K27ac⁵³, disrupting metabolism (S1P accumulation impairing IL-15-dependent survival⁵¹, mitochondrial ROS activating Caspase-3/9-mediated apoptosis⁵⁰), and inducing immune checkpoints (WDR5-mediated H3K4me3 upregulated PD-L1 and HLA-E, engaging NK inhibitory receptors PD-1 and NKG2A^{31,52}). In HBV-associated HCC, this mechanism impaired the release of perforin/granzyme and reduced IFN- γ secretion, hindering direct tumor cell killing and impeding M1 macrophage polarization/DC antigen presentation. Concurrently, it reduced Fas/FasL-mediated clearance of infected hepatocytes, thereby accelerating malignant transformation [33]. YEATS2 also inhibits mast cell infiltration, disrupting their functional balance: suppressing tumor-restrictive activity (chymase-mediated angiotensin II inducing fibrotic encapsulation) while potentially augmenting protumor

effects (tryptase activating PAR2 to stimulate VEGF/IL-6 and MMP-9). Furthermore, YEATS2 may impair spatial distribution via CXCL12/CXCR4 axis perturbation, potentially exacerbating histamine/STAT3-mediated enhancement of cancer stemness [34]. The concordance of YEATS2 knockdown with increased NK infiltration and tumor regression in xenografts validates this metabolic-epigenetic-immune regulatory axis [11].

Elevated YEATS2 expression potentially enhanced anti-PD-L1 immunotherapy efficacy by augmenting monocyte infiltration and their differentiation into PD-L1 + TAMs. This process paradoxically fostered immunosuppression while simultaneously sensitizing tumors to PD-L1 blockade. YEATS2 inversely correlated with mast cell infiltration, suggesting therapeutic synergy since mast cell modulation combined with anti-PD-1 improved HCC outcomes⁵⁴. YEATS2 exhibited strong co-expression with TGFBR1-where its inhibition reduced proliferation⁵⁵ while activation promoted EMT-mediated invasion⁵⁶ -and with the immune checkpoint TIGIT. TIGIT synergized with PD-L1 to suppress T/NK cell activity and promote immune escape^{57,58}, explaining the potent efficacy of dual TIGIT/PD-1/PD-L1 targeting⁵⁹ and aligning with YEATS2-mediated anti-PD-L1 sensitivity.

YEATS2 upregulates chemokines CCL20 (promoting migration/proliferation⁶⁰ and immune evasion⁶¹), CXCL5 (a serum biomarker stimulating tumor growth^{62,63} and neutrophil recruitment⁶⁴), and CCL28 (modulating T cell/macrophage trafficking⁶⁵), collectively promoting HCC progression. High YEATS2 levels also reduced sorafenib response by driving EMT-mediated resistance via non-coding RNA pathways and E-cadherin/N-cadherin dysregulation^{66,67}. Conversely, YEATS2 knockdown elevated hepatic NK cell infiltration¹¹, and enhanced NK activity correlated positively with sorafenib efficacy³³, highlighting YEATS2's dual role in modulating immunotherapy and targeted therapy responses.

The established oncogenic role of YEATS2 in HCC presents significant clinical opportunities, including its utility as an accessible serum biomarker via standardized ELISA protocols for diagnosis and prognosis prediction, the therapeutic potential of the YEATS2-WDR5 axis revealed by bioinformatics analyses, and its correlation with enhanced anti-PD-L1 response enabling combination strategies and patient stratification based on NK cell links, though YEATS2-mediated countereffects on fatty acid metabolism complicate statin repurposing. Despite validation from public cohorts and in vivo evidence of tumor suppression from knockout studies¹¹, limited sample sizes and reliance on in vitro models underscore the urgent need for large-scale multicenter clinical validation to define serum thresholds and comprehensive in vivo studies to confirm functional roles in metastasis and microenvironment modulation. Future efforts must prioritize these steps to fully harness YEATS2's biomarker and therapeutic potential in HCC.

Conclusions

This study establishes YEATS2 as a pivotal orchestrator of HCC pathogenesis, driving tumor progression through dual chemoresistance and immunomodulatory mechanisms. Clinically, elevated YEATS2 expression serves as both a prognostic biomarker for aggressive disease and a predictive indicator of enhanced anti-PD-L1 therapeutic response. The paradoxical association between YEATS2-mediated immunosuppression and PD-L1 blockade sensitivity reveals a targetable vulnerability in high-risk HCC, offering a precision medicine strategy for tumors refractory to conventional therapies.

Data availability

The datasets used and analyzed during the current study are available from the corresponding author upon reasonable request.

Received: 24 September 2024; Accepted: 1 July 2025

Published online: 29 July 2025

References

1. Siegel, R. L., Miller, K. D., Wagle, N. S. & Jemal, A. Cancer statistics, 2023. *Cancer J. Clin.* **73** (1), 17–48 (2023).
2. Villanueva, A. Hepatocellular carcinoma. *N. Engl. J. Med.* **380** (15), 1450–1462 (2019).
3. Liu, J. et al. Immunotherapy, targeted therapy, and their cross talks in hepatocellular carcinoma. *Front. Immunol.* **14**, 1285370 (2023).
4. Wang, Q. et al. The YEATS domain histone crotonylation readers control Virulence-Related biology of a major human pathogen. *Cell. Rep.* **31** (3), 107528 (2020).
5. Xia, J. K. et al. Roles and regulation of histone acetylation in hepatocellular carcinoma. *Front. Genet.* **13**, 982222 (2022).
6. Mi, W. et al. YEATS2 links histone acetylation to tumorigenesis of non-small cell lung cancer. *Nat. Commun.* **8** (1), 1088 (2017).
7. Sheng, H. et al. YEATS2 regulates the activation of TAK1/NF- κ B pathway and is critical for pancreatic ductal adenocarcinoma cell survival. *Cell. Biol. Toxicol.* **39** (3), 1–16 (2023).
8. Sha, T. et al. YEATS domain-containing 2 (YEATS2), targeted by MicroRNA miR-378a-5p, regulates growth and metastasis in head and neck squamous cell carcinoma. *Bioengineered* **12** (1), 7286–7296 (2021).
9. Long, Y., Wang, W., Liu, S., Wang, X. & Tao, Y. The survival prediction analysis and preliminary study of the biological function of YEATS2 in hepatocellular carcinoma. *Cell. Oncol. (Dordrecht Netherlands)*. **47** (6), 2297–2316 (2024).
10. Liu X, Hu Y, Li C, Chen J, Liu X, Shen Y, Xu Y, Chen W, Xu X. Overexpression of YEATS2 Remodels the Extracellular Matrix to Promote Hepatocellular Carcinoma Progression via the PI3K/AKT Pathway. *Cancers (Basel)*. 2023 Mar 20;15(6):1850.
11. Wu, Q. et al. Repression of YEATS2 induces cellular senescence in hepatocellular carcinoma and inhibits tumor growth. *Cell. Cycle (Georgetown Tex)*. **23** (4), 478–494 (2024).
12. Liberzon, A. et al. Molecular signatures database (MSigDB) 3.0. *Bioinf. (Oxford England)*. **27** (12), 1739–1740 (2011).
13. Blum, A., Wang, P. & Zenklusen, J. C. SnapShot: TCGA-Analyzed tumors. *Cell* **173** (2), 530 (2018).
14. Love, M. I., Huber, W. & Anders, S. Moderated Estimation of fold change and dispersion for RNA-seq data with DESeq2. *Genome Biol.* **15** (12), 550 (2014).
15. Liu, Z. et al. BEST: a web application for comprehensive biomarker exploration on large-scale data in solid tumors. *J. Big Data.* **10** (1), 165 (2023).

16. Shi, Y. et al. Role of IQGAP3 in metastasis and epithelial-mesenchymal transition in human hepatocellular carcinoma. *J. Transl. Med.* **15** (1), 176 (2017).
17. Szklarczyk, D. et al. STRING v10: protein-protein interaction networks, integrated over the tree of life. *Nucleic Acids Res.* **43** (Database issue), D447–452 (2015).
18. Doncheva, N. T., Morris, J. H., Gorodkin, J. & Jensen, L. J. Cytoscape stringapp: network analysis and visualization of proteomics data. *J. Proteome Res.* **18** (2), 623–632 (2019).
19. Kanehisa, M. & Goto, S. KEGG: Kyoto encyclopedia of genes and genomes. *Nucleic Acids Res.* **28** (1), 27–30 (2000).
20. Kanneganti M, Al-Hasan M, Bourque S, Deodhar S, Yang JD, Huang DQ, Kulkarni AV, Gopal P, Parikh ND, Kanwal F, Patel MS, Singal AG. Older Age But Not Comorbidity Is Associated With Worse Survival in Patients With Hepatocellular Carcinoma. *Clin Gastroenterol Hepatol.* 2025 Jul;23(8):1377–1386.e2.
21. Cullaro, G., Rubin, J. B., Mehta, N. & Lai, J. C. Differential impact of age among liver transplant candidates with and without hepatocellular carcinoma. *Liver Transplantation: Official Publication Am. Association Study Liver Dis. Int. Liver Transplantation Soc.* **26** (3), 349–358 (2020).
22. Jain, S. S., McNamara, M. E., Varghese, R. S. & Ransom, H. W. Deconvolution of immune cell composition and biological age of hepatocellular carcinoma using DNA methylation. *Methods (San Diego Calif.)*. **218**, 125–132 (2023).
23. Yu H, Jin S, Zeng M, Yang Z, Wang X. TIGIT antibody with PVR competitive ability enhances cancer immunotherapy and capable of eliciting anti-tumour immune memory. *Br J Cancer.* 2025 May 20. doi: 10.1038/s41416-025-03046-w. Epub ahead of print. PMID: 40394151.
24. Zhang, N. et al. Novel therapeutic strategies: targeting epithelial-mesenchymal transition in colorectal cancer. *Lancet Oncol.* **22** (8), e358–e368 (2021).
25. Xue, W. et al. BPA modulates the WDR5/TET2 complex to regulate ER β expression in eutopic endometrium and drives the development of endometriosis. *Environmental pollution (Barking, Essex.)* 2021, 268(Pt B):115748. 2021, 268(Pt B):115748. (1987).
26. Zhang, Y., Zhang, H. & Wu, S. LncRNA-CCDC144NL-AS1 promotes the development of hepatocellular carcinoma by inducing WDR5 expression via sponging miR-940. *J. Hepatocellular Carcinoma.* **8**, 333–348 (2021).
27. Kent, L. N. & Leone, G. The broken cycle: E2F dysfunction in cancer. *Nat. Rev. Cancer.* **19** (6), 326–338 (2019).
28. Oshi M, Takahashi H, Tokumaru Y, Yan L, Rashid OM, Matsuyama R, Endo I, Takabe K. G2M Cell Cycle Pathway Score as a Prognostic Biomarker of Metastasis in Estrogen Receptor (ER)-Positive Breast Cancer. *Int J Mol Sci.* 2020 Apr 22;21(8):2921.
29. Currie, E., Schulze, A., Zechner, R., Walther, T. C. & Farese, R. V. Jr. Cellular fatty acid metabolism and cancer. *Cell Metabol.* **18** (2), 153–161 (2013).
30. Massart J, Begriche K, Corlu A, Fromenty B. Xenobiotic-Induced Aggravation of Metabolic-Associated Fatty Liver Disease. *Int J Mol Sci.* 2022 Jan 19;23(3):1062.
31. Zhang, Z. et al. Wdr5-mediated H3K4me3 coordinately regulates cell differentiation, proliferation termination, and survival in digestive organogenesis. *Cell. Death Discovery.* **9** (1), 227 (2023).
32. Chen X, Li Y, Xia H, Chen YH. Monocytes in Tumorigenesis and Tumor Immunotherapy. *Cells.* 2023 Jun 21;12(13):1673.
33. Sajid, M., Liu, L. & Sun, C. The dynamic role of NK cells in liver cancers: role in HCC and HBV associated HCC and its therapeutic implications. *Front. Immunol.* **13**, 887186 (2022).
34. Huang, S. et al. Exploring the role of mast cells in the progression of liver disease. *Front. Physiol.* **13**, 964887 (2022).
35. Theoharides, T. C. & Conti, P. Mast cells: the Jekyll and Hyde of tumor growth. *Trends Immunol.* **25** (5), 235–241 (2004).
36. Yang, D., Du, J., Nie, W., Wang, C. & Ma, Z. Combination treatment of transcatheter arterial chemoembolization, intensity-modulated radiotherapy, and Sorafenib for hepatocellular carcinoma with macrovascular invasion. *Medicine* **102** (45), e35713 (2023).
37. Zhang, C., Xu, C., Gao, X. & Yao, Q. Platinum-based drugs for cancer therapy and anti-tumor strategies. *Theranostics* **12** (5), 2115–2132 (2022).
38. Kotsari M, Dimopoulou V, Koskinas J, Armakolas A. Immune System and Hepatocellular Carcinoma (HCC): New Insights into HCC Progression. *Int J Mol Sci.* 2023 Jul 14;24(14):11471.
39. Peng, F., Zhu, F., Cao, B. & Peng, L. Multidimensional analysis of PANoptosis-Related molecule CASP8: prognostic significance, immune microenvironment effect, and therapeutic implications in hepatocellular carcinoma. *Genet. Res.* **2023**, 2406193 (2023).
40. Wang, Y. L., Faiola, F., Xu, M., Pan, S. & Martinez, E. Human ATAC is a GCN5/PCAF-containing acetylase complex with a novel NC2-like histone fold module that interacts with the TATA-binding protein. *J. Biol. Chem.* **283** (49), 33808–33815 (2008).
41. Jeon, T., Oh, U. J., Min, J. & Kim, C. Gene-level dissection of chromosome 3q locus amplification in squamous cell carcinoma of the lung using the nCounter assay. *Thorac. Cancer.* **14** (26), 2635–2641 (2023).
42. Lan, T. et al. Cinobufacini retards progression of pancreatic ductal adenocarcinoma through targeting YEATS2/TAK1/NF- κ B axis. *Phytomedicine* **109**, 154564 (2023).
43. Qu, Q., Zeng, F., Liu, X., Wang, Q. J. & Deng, F. Fatty acid oxidation and carnitine palmitoyltransferase I: emerging therapeutic targets in cancer. *Cell. Death Dis.* **7** (5), e2226 (2016).
44. Chiang, I. T. et al. Hyperforin inhibits cell growth by inducing intrinsic and extrinsic apoptotic pathways in hepatocellular carcinoma cells. *Anticancer Res.* **37** (1), 161–167 (2017).
45. Nowak, A. K., Stockler, M. R., Chow, P. K. & Findlay, M. Use of Tamoxifen in advanced-stage hepatocellular carcinoma. A systematic review. *Cancer* **103** (7), 1408–1414 (2005).
46. Shou, J. et al. Mechanisms of Tamoxifen resistance: increased Estrogen receptor-HER2/neu cross-talk in ER/HER2-positive breast cancer. *J. Natl. Cancer Inst.* **96** (12), 926–935 (2004).
47. Goh, M. J. & Sinn, D. H. Statin and aspirin for chemoprevention of hepatocellular carcinoma: time to use or wait further? *Clin. Mol. Hepatol.* **28** (3), 380–395 (2022).
48. Park, J. H. et al. Statin prevents cancer development in chronic inflammation by blocking Interleukin 33 expression. *Nat. Commun.* **15** (1), 4099 (2024).
49. Wang, E., Sun, S., Li, H., Jia, Y. & Bai, Z. HBx/WDR5 enhances IGF-1 transcription in hepatocellular carcinoma cells and promotes recruitment, infiltration, and activity of Treg cells. *Immunol. Res.* **73** (1), 69 (2025).
50. Xiong, J. et al. Lactylation-driven METTL3-mediated RNA m(6A) modification promotes immunosuppression of tumor-infiltrating myeloid cells. *Mol. Cell.* **82** (9), 1660–1677.e1610 (2022).
51. Chu, X., Zhang, Y. & Cheng, S. Heterogeneity of tumor-infiltrating myeloid cells in era of single-cell genomics. *Chin. J. cancer Res. = Chung-kuo Yen Cheng Yen Chiu.* **34** (6), 543–553 (2022).
52. Zhang, Y. & Zhang, Z. The history and advances in cancer immunotherapy: Understanding the characteristics of tumor-infiltrating immune cells and their therapeutic implications. *Cell Mol. Immunol.* **17** (8), 807–821 (2020).
53. Song, J. et al. PTIR1 acts as an isoform of DDX58 and promotes tumor immune resistance through activation of UCHL5. *Cell. Rep.* **42** (11), 113388 (2023).
54. Fridman, W. H., Pagès, F., Sautès-Fridman, C. & Galon, J. The immune contexture in human tumours: impact on clinical outcome. *Nat. Rev. Cancer.* **12** (4), 298–306 (2012).
55. Fabregat, I. & Caballero-Díaz, D. Transforming growth Factor- β -Induced cell plasticity in liver fibrosis and hepatocarcinogenesis. *Front. Oncol.* **8**, 357 (2018).
56. Moustakas A, Heldin CH. Mechanisms of TGF β -Induced Epithelial-Mesenchymal Transition. *J Clin Med.* 2016 Jun 29;5(7):63.
57. Joller, N. et al. Cutting edge: TIGIT has T cell-intrinsic inhibitory functions. *J. Immunol.* **186** (3), 1338–1342 (2011).

58. Chauvin, J. M. et al. TIGIT and PD-1 impair tumor antigen-specific CD8⁺ T cells in melanoma patients. *J. Clin. Invest.* **125** (5), 2046–2058 (2015).
59. Zheng, Q. et al. Immune checkpoint targeting TIGIT in hepatocellular carcinoma. *Am. J. Translational Res.* **12** (7), 3212–3224 (2020).
60. Rubie, C. et al. Enhanced expression and clinical significance of CC-chemokine MIP-3 alpha in hepatocellular carcinoma. *Scand. J. Immunol.* **63** (6), 468–477 (2006).
61. Campbell, J. J. & Butcher, E. C. Chemokines in tissue-specific and microenvironment-specific lymphocyte homing. *Curr. Opin. Immunol.* **12** (3), 336–341 (2000).
62. Xu, X., Huang, P., Yang, B., Wang, X. & Xia, J. Roles of CXCL5 on migration and invasion of liver cancer cells. *J. Transl. Med.* **12**, 193 (2014).
63. Laschtowitz A, Lambrecht J, Puengel T, Tacke F, Mohr R. Serum CXCL5 Detects Early Hepatocellular Carcinoma and Indicates Tumor Progression. *Int J Mol Sci.* 2023 Mar 10;24(6):5295.
64. Zhou, S. L. et al. Overexpression of CXCL5 mediates neutrophil infiltration and indicates poor prognosis for hepatocellular carcinoma. *Hepatology* **56** (6), 2242–2254 (2012).
65. Ren, L. et al. Hypoxia-induced CCL28 promotes recruitment of regulatory T cells and tumor growth in liver cancer. *Oncotarget* **7** (46), 75763–75773 (2016).
66. Xu, J. et al. N(6)-methyladenosine-modified CircRNA-SORE sustains Sorafenib resistance in hepatocellular carcinoma by regulating β -catenin signaling. *Mol. Cancer.* **19** (1), 163 (2020).
67. Xia, S., Pan, Y., Liang, Y., Xu, J. & Cai, X. The microenvironmental and metabolic aspects of Sorafenib resistance in hepatocellular carcinoma. *EBioMedicine* **51**, 102610 (2020).

Acknowledgements

Deepseek was used solely for language polishing and did not contribute to any creative knowledge generation. And we sincerely thank Kanehisa Laboratories for granting permission to use KEGG pathway data in this study.

Author contributions

SH, YC, and HJ: Conceived the study, designed the experiments, and provided administrative support. YS and QX: Contributed equally to the preparation of the manuscript. All authors: Contributed study materials, conducted in vitro cell experiments, conducted literature research, collected, analyzed, and interpreted data, and approved the final manuscript.

Funding

This work was supported by the Guangdong Medical Science and Technology Research Fund Project [grant No. A2023165], and the Guangzhou Health Science and Technology Project [grant No. 20251A011074].

Declarations

Competing interests

The authors declare no competing interests.

Additional information

Supplementary Information The online version contains supplementary material available at <https://doi.org/10.1038/s41598-025-09945-5>.

Correspondence and requests for materials should be addressed to H.J., Y.C. or S.H.

Reprints and permissions information is available at www.nature.com/reprints.

Publisher's note Springer Nature remains neutral with regard to jurisdictional claims in published maps and institutional affiliations.

Open Access This article is licensed under a Creative Commons Attribution-NonCommercial-NoDerivatives 4.0 International License, which permits any non-commercial use, sharing, distribution and reproduction in any medium or format, as long as you give appropriate credit to the original author(s) and the source, provide a link to the Creative Commons licence, and indicate if you modified the licensed material. You do not have permission under this licence to share adapted material derived from this article or parts of it. The images or other third party material in this article are included in the article's Creative Commons licence, unless indicated otherwise in a credit line to the material. If material is not included in the article's Creative Commons licence and your intended use is not permitted by statutory regulation or exceeds the permitted use, you will need to obtain permission directly from the copyright holder. To view a copy of this licence, visit <http://creativecommons.org/licenses/by-nc-nd/4.0/>.

© The Author(s) 2025